

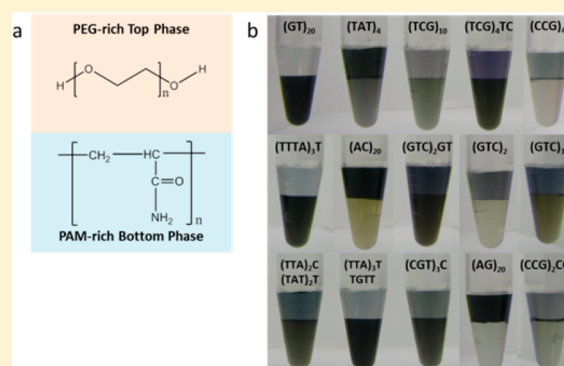
# DNA-Controlled Partition of Carbon Nanotubes in Polymer Aqueous Two-Phase Systems

Geyou Ao, Constantine Y. Khripin, and Ming Zheng\*

Materials Science and Engineering Division, National Institute of Standards and Technology, 100 Bureau Drive, Gaithersburg, Maryland 20899, United States

**S** Supporting Information

**ABSTRACT:** Sorting single-wall carbon nanotubes (SWCNTs) of different chiralities is both scientifically interesting and technologically important. Recent studies have shown that polymer aqueous two-phase extraction is a very effective way to achieve nanotube sorting. However, works published to date have demonstrated only separation of surfactant-dispersed SWCNTs, and the mechanism of chirality-dependent SWCNT partition is not well understood. Here we report a systematic study of spontaneous partition of DNA-wrapped SWCNTs in several polymer aqueous two-phase systems. We show that partition of DNA–SWCNT hybrids in a given polymer two-phase system is strongly sequence-dependent and can be further modulated by salt and polymer additives. With the proper combination of DNA sequence, polymer two-phase system, and partition modulators, as many as 15 single-chirality nanotube species have been effectively purified from a synthetic mixture. As an attempt to provide a unified partition mechanism of SWCNTs dispersed by surfactants and by DNA, we present a qualitative analysis of solvation energy for SWCNT colloids in a polymer-modified aqueous phase. Our observation and analysis highlight the sensitive dependence of the hydration energy on the spatial distribution of hydrophilic functionalities.



## INTRODUCTION

An efficient and robust method for the purification of single-wall carbon nanotubes (SWCNTs) utilizing a polymer aqueous two-phase (ATP) system has been demonstrated recently<sup>1–4</sup> and shows some unique advantages over other reported separation schemes.<sup>5–11</sup> The ATP extraction method, pioneered by Albertson,<sup>12</sup> uses the phenomenon of polymer–polymer phase separation to create two immiscible aqueous phases with slightly different physical properties. For a given analyte, any difference in solvation energy leads to its uneven distribution in the two phases. This provides a mechanism for sorting complex mixtures of analytes. A robust example is the spontaneous partition of surfactant-dispersed SWCNTs across the immiscible aqueous phases of dextran (DX) and poly(ethylene glycol) (PEG), which has enabled purification of metallic, semiconducting, and single-chirality enriched SWCNTs.<sup>1,2</sup> In addition to its technological implications, we believe SWCNT partition in ATP systems provides a useful experimental model system to study macromolecular behavior in aqueous phases. Specifically, colloidal SWCNTs have well-defined geometries and easily controlled surface functionalization, making it possible to experimentally explore how the solvation energy of a biomacromolecule-like object scales with its dimensions<sup>13,14</sup> and varies with the distribution of surface functionalities—a fundamental issue in biophysics.

Previous works on ATP separation of SWCNTs have been limited to their surfactant dispersions.<sup>1–4</sup> The extensive selection of aqueous polymer systems<sup>12,15</sup> and their use in the purification of biomolecules<sup>12,16</sup> motivated us to extend the ATP method to the separation of SWCNTs dispersed by non-surfactant-type molecules such as DNA, peptides,<sup>17–19</sup> and other polymers.<sup>10,20</sup> Of particular interest to us are SWCNTs dispersed by single-stranded DNA (DNA-SWCNTs).<sup>5–8</sup> The size of the single-stranded DNA (ssDNA) library allows for a practically unlimited number of ways to coat SWCNTs. Effective separation of DNA-SWCNTs will provide a foundation for many fundamental studies and potential biomedical applications of SWCNTs. Previous studies of the separation of DNA-SWCNTs using ion-exchange chromatography (IEX) have identified more than 20 recognition DNA sequences within the length of 40-mers for sorting semiconducting SWCNT (*n,m*) species<sup>5</sup> and armchair metallic (6,6) and (7,7) species.<sup>6</sup> The basis of DNA recognition of SWCNTs, which is the subject of many current studies,<sup>21–24</sup> may involve the formation of a well-ordered DNA structure around one particular (*n,m*) species through inter- and intrastrand hydrogen bonding. It is hypothesized that the structurally well-defined hybrid enables the elution of the target SWCNT

Received: April 24, 2014

Published: June 28, 2014

species at a defined and earlier time as a result of its weaker electrostatic, van der Waals, and hydrophobic interactions with the positively charged IEX resin. Since IEX involves complicated molecular interactions in heterogeneous phases, it is rather difficult to achieve a quantitative understanding of the separation process. In contrast, ATP separation occurs in well-defined and tunable homogeneous solutions. The process should be more amenable to quantitative analysis in terms of molecular interactions.

In this contribution, we report a systematic study of DNA-SWCNT separation by the ATP method. Strong sequence-dependent partition of DNA-SWCNTs has been observed. Because of the enormous size of the ssDNA library, it was practical for us to examine only a small number of DNA sequences for separation. Thus, we limited our sequence choice mainly to SWCNT-recognition DNA sequences previously identified via IEX. Nevertheless, this small number of sequences allowed us to purify 15 metallic and semiconducting ( $n,m$ ) species from a starting SWCNT synthetic mixture using the ATP method. These results expand the utility as well as our understanding of the mechanism of ATP separation of SWCNTs. For surfactant-dispersed SWCNTs, partition is strongly correlated with the diameter and metal/semiconductor nature of the SWCNTs, and the influence of the surfactant structure is not readily discernible. In contrast, partition of DNA-SWCNTs is primarily dependent on the sequence of the coating DNA. As a first attempt to reach a unified description of partition in ATP of both surfactant- and DNA-dispersed SWCNTs, we provide a discussion of the solvation energy of a colloidal SWCNT in terms of its physical characteristics (diameter, length, chirality) and distribution of surface functionalities.

## MATERIALS AND METHODS

CoMoCAT SWCNT powders (SG65 grade, lot no. SG65EX-002, and SG65i grade, lot no. SG65i-L46) were obtained from Southwest Nanotechnologies. Custom-made DNA was purchased from Integrated DNA Technologies. Dextran 70 (DX, MW  $\sim$ 70 kDa, TCI), PEG (MW 6 kDa, Alfa Aesar), poly(vinylpyrrolidone) (PVP, MW 10 kDa, Sigma-Aldrich), polyacrylamide (PAM, 10 kDa, Sigma-Aldrich), poly(ethylene glycol) diamine (PEG-DA, MW 6 kDa, Scientific Polymer Products, Inc.), sodium chloride (NaCl, BDH Chemicals), and sodium thiocyanate (NaSCN, Sigma-Aldrich) were used as received.

For dispersion of SWCNTs with a given DNA sequence, a total volume of 1 mL of the DNA and SWCNT mixture in deionized (DI) water with 0.1 mol/L NaCl was sonicated in an ice bath (model VCX 130, Sonics and Materials, Inc.) for 2 h at a power level of 8 W. Typically, the SWCNT/DNA mass ratio was 1:2, but a 1:4 ratio was used for some of the short DNA sequences. The DNA concentration was kept constant at 2 mg/mL. After centrifugation at 17000g for 90 min, the supernatant of the DNA-SWCNT dispersion was collected and used for the ATP separation at room temperature ( $20 \pm 1^\circ\text{C}$ ). The compositions of the ATP systems are listed in Table 1. Typically, partition of SWCNTs in the two immiscible aqueous phases was obtained by vortex mixing of the mixture of DNA-SWCNTs and immiscible polymers in a microcentrifuge tube for 1 min followed by centrifugation at 9000g for 1–2 min. In the case of the PEG/PAM system, overnight incubation of the mixture led to improved yield and purity of ( $n,m$ ) species after the first step of separation, while for the (PEG + PEG-DA)/DX system, the separation was carried out immediately to avoid excess aggregation of nanotubes. Detailed procedures for the purification of each ( $n,m$ ) species are described in the Supporting Information (Tables S1 and S2 and other detailed descriptions).

Table 1. ATP Systems Used in This Work

ATP system	polymer, MW	mass %
PEG/PAM	PEG, 6 kDa	7.76
	PAM, 10 kDa	15.0
PEG/DX	PEG, 6 kDa	5.50
	DX, 70 kDa	7.50
(PEG + PEG-DA)/DX	PEG, 6 kDa	2.75
	PEG-DA, 6 kDa	2.75
	DX, 70 kDa	7.50
PVP/DX	PVP, 10 kDa	16.0
	DX, 70 kDa	11.0

UV–vis–NIR absorbance measurements were performed on a Varian Cary 5000 spectrophotometer over the wavelength range of 200–1400 nm using a 10 mm path length quartz microcuvette. SWCNT fractions in polymer solutions were diluted for UV–vis–NIR measurements, and each absorbance value was multiplied by the dilution factor to obtain the true absorbance of the original solution. Blank top or bottom phases of ATP systems without SWCNTs were diluted in the same way as the corresponding SWCNT fractions for baseline measurements. For purified metallic SWCNTs, polymers and impurities were further removed from the sample by a previously reported SWCNT precipitation method<sup>25</sup> to allow resolution of nanotube absorption features in the UV region. Specifically, NaSCN was added to the isolated metallic species in the either DX-rich or PAM-rich bottom phase to a final concentration of 1.5 mol/L, and the mixture was incubated overnight at 4 °C and then centrifuged at 17000g for 30 min. A similar procedure was used to precipitate semiconducting SWCNT ( $n,m$ ) species isolated in the PEG-rich top phase, except a shorter centrifugation at 17000g for 5 min was found to be sufficient. After centrifugation, the supernatant was removed and the pellet was resuspended in water.

## RESULTS AND DISCUSSION

**Sequence-Dependent Partition.** The most important observation of this work is that partition of DNA-SWCNTs in an ATP system is strongly sequence-dependent. Here we use SWCNT partition in the PEG/PAM system (Figure 1) as an example to illustrate the observations. For some sequences, such as (GT)<sub>20</sub>, SWCNTs primarily settle in the more hydrophilic PAM-rich bottom phase; for others, such as (AG)<sub>20</sub>, the nanotubes are predominantly distributed into the more hydrophobic PEG-rich top phase. Lastly, for sequences such as (GTC)<sub>3</sub>, approximately equal amounts of SWCNTs are partitioned into the two phases, but with different ( $n,m$ ) distributions. Overall, the variation of SWCNT partition as a function of the DNA sequence could be easily observed by the naked eye and could be shown even more strikingly with optical absorption measurements. If we view SWCNT partition in PEG/PAM as a “phenotype” determined by a single “gene” that specifies the SWCNT-wrapping DNA sequence, then what we have created here can be called a “single-gene molecular system”—an assembly of many interacting molecules that can be programmed to exhibit certain spatial organization and physicochemical properties. In comparison, a living cell is a molecular system containing thousands of genes.

DNA-sequence-dependent partition implies that the solvation energy of a DNA-SWCNT in a polymer-modified aqueous phase is sensitive to the coating DNA. This is not surprising in light of previous studies showing sequence-dependent outcomes of IEX separation<sup>5,6</sup> and sequence-dependent wrapping of DNA on SWCNTs. Manifestation of the sequence dependence in an ATP system is additionally dependent on the solvation energy difference between the two phases. In the

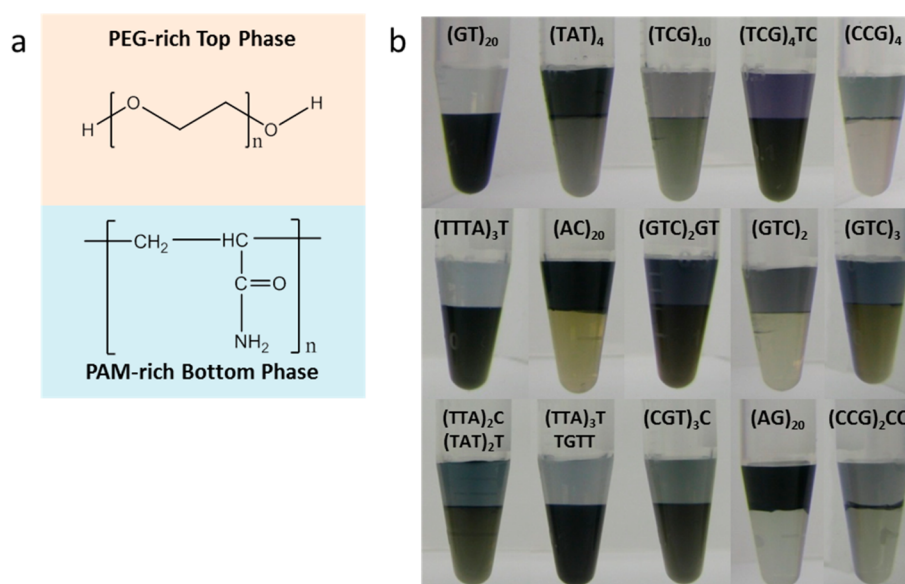
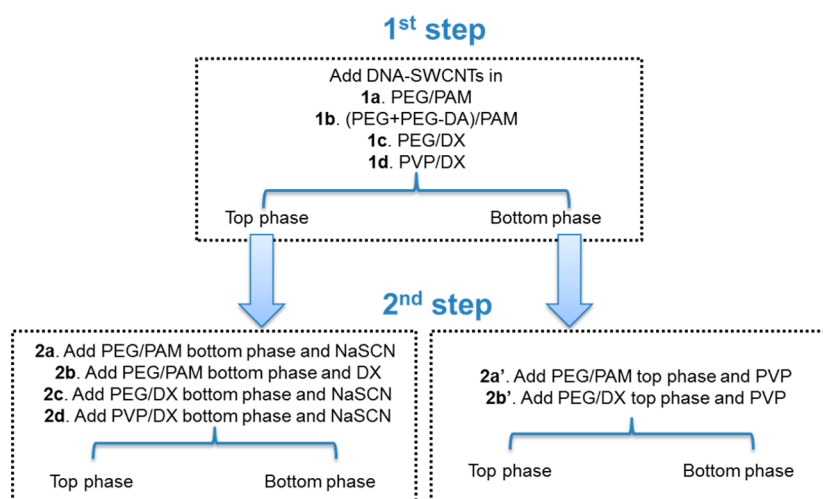


**Figure 1.** Sequence-dependent partition of DNA-SWCNTs in the PEG/PAM system. (a) Schematic of the PEG/PAM system, in which the top phase is PEG-rich and the bottom phase is PAM-rich. (b) Photographs showing the partition of various DNA-SWCNTs in the PEG/PAM system. For each vial, the DNA sequence used for SWCNT dispersion is labeled on the sidewall. A volume of 25  $\mu\text{L}$  (smaller than that used in real separation) of stock DNA-SWCNT dispersion was added to 475  $\mu\text{L}$  of the PEG/PAM system for the photograph.

### Scheme 1. Flowchart for ATP Separation of DNA-SWCNTs



PEG/DX system, for example, SWCNTs wrapped by all sequences tested preferred the DX-rich bottom phase, showing much less apparent sequence-dependent partition. This observation is probably caused by a larger difference in hydrophobicity/hydrophilicity between the two immiscible phases in PEG/DX than in PEG/PAM.

**Multiple Choice of ATP Systems.** In comparison with the surfactant-dispersed SWCNTs, DNA-SWCNTs were found to be compatible with more ATP systems, most likely because of their surfactant-free nature and higher colloidal stability. Partition of a given DNA-SWCNT dispersion was found to be dependent on the choice of ATP system. This observation proved to be very useful in fractionating SWCNT mixtures, since different ATP systems can be used at different stages in sequence to achieve enrichment of a targeted  $(n,m)$  species. Three ATP systems were mainly used in this work: PEG/PAM, (PEG + PEG-DA)/DX, and PVP/DX. PEG-DA, which has amine groups that can be protonated to bear positive charge,

was employed for its ability to introduce an electrostatic-based separation mechanism. Indeed, we found that in the (PEG + PEG-DA)/DX system, a substantial amount of SWCNTs were moved to the top phase in comparison with the pristine PEG/DX system, presumably as a result of the electrostatic interactions between the positively charged PEG-DA and negatively charged DNA-SWCNT hybrids. The PEG/DX system is compatible with DNA-SWCNTs. However, the DX-enriched bottom phase has very high affinity for DNA-SWCNTs, making the PEG/DX system less effective than the other three ATP systems for purifying single  $(n,m)$  species. The PVP/PAM and PEG/PVP two-phase systems form at relatively high polymer concentrations, and the resulting high viscosity of these systems hinders the partition of DNA-SWCNTs, rendering them less useful.

**Modulation of DNA-SWCNT Partition.** DNA-SWCNT partition in any given ATP system could be additionally modulated in a number of ways, including addition of polymer

or salt and adjustment of the pH. Generally speaking, adding PVP or a kosmotropic salt [e.g.,  $(\text{NH}_4)_2\text{SO}_4$  or  $\text{Na}_2\text{CO}_3$ ] or raising the pH by adding NaOH drives nanotubes to the more hydrophobic top phase, while adding DX or a chaotropic salt (e.g., NaSCN) pushes nanotubes to the more hydrophilic bottom phase.

While these partition modulators proved to be extremely useful for SWCNT separation, the mechanisms by which they function are not well understood. The opposite roles played by chaotropic and kosmotropic salts are not surprising in light of the well-documented and ubiquitous Hofmeister effect.<sup>26</sup> The observed modulation effect of PVP, however, resembles no other cases. PVP is one of a few water-soluble polymers mentioned in Albertsson's original book on ATP.<sup>12</sup> In the course of this work, we discovered that PVP is extremely effective in increasing SWCNT partition into the top phase. The molecular structure of PVP consists of a hydrophobic backbone with hydrophilic side chains, and PVP can form ATP systems with several other polymers.<sup>15</sup> It has been reported that PVP may carry positive charge to interact strongly with anionic surfactant-dispersed SWCNTs.<sup>27</sup> PVP alone can also solubilize SWCNTs in water.<sup>20</sup> Most interestingly, PVP is reported to behave like a kosmotropic salt in aqueous solution.<sup>28</sup> This certainly is consistent with our observation that PVP acts similarly to  $(\text{NH}_4)_2\text{SO}_4$  and  $\text{Na}_2\text{CO}_3$ . Therefore, the mechanism of PVP modulation of DNA-SWCNT partition may involve changes in water structure due to the kosmotropic nature of PVP.

**General Separation Strategy.** Multiple choices of DNA sequences, ATP systems, and partition modulators form a large toolbox for developing DNA-SWCNT fractionation strategies. Scheme 1 outlines a general procedure we designed for multistep separation. For each step, a few of the aforementioned options are listed in the scheme. In general, DNA-SWCNTs were mixed with an ATP system in the first step of separation. Different ATP systems yield different SWCNT partitions. For the second step of separation, an equal volume of blank opposite phase was added to the volume of the target fraction containing SWCNTs to form a new ATP system. In addition, an appropriate amount of modulating agent was added in the new ATP system to obtain a new SWCNT partition. The entire second step can be repeated multiple times in order to achieve a desirable separation outcome. Table 2 summarizes the ATP system(s) and DNA sequences used for each  $(n,m)$  species purified. In those cases where two or more DNA sequences enabled the purification of an  $(n,m)$  species, the first DNA sequence listed provided more effective separation of the  $(n,m)$  species according to the experimental conditions used in this work. The purification yield given in Table 2 for each  $(n,m)$  species corresponds to the first DNA sequence listed. It is based on the ratio of the mass of purified  $(n,m)$  species to the total mass of SWCNTs used for the ATP separation (see the Supporting Information for details). In general, the yield of the ATP method is at least 3–4 times higher than that of the IEX method for any given  $(n,m)$  species. In what follows, we present some specific examples of executing the general strategy for SWCNT purification. More examples can be found in the Supporting Information.

**Total Fractionation of SWCNTs Dispersed by a Given DNA Sequence.** Following Scheme 1 enables the total fractionation of a SWCNT dispersion made by any given sequence. A schematic illustration of multistep separation of  $(\text{GT})_{20}$ -SWCNTs in the PEG/PAM system is shown in Figure

**Table 2. DNA Sequence(s) and ATP System(s) Used for Each Purified  $(n,m)$  Species**

chirality $(n,m)$	DNA sequence	yield (mass %)	ATP system
(5,5)	$(\text{GT})_{20}$	0.5	PEG/PAM
(7,4)	$(\text{GT})_{20}$	0.4	
(8,4)	$(\text{GT})_{20}$	2.7	
(7,5)	$(\text{TATT})_3\text{T}, (\text{GTT})_3\text{G}$	4.9	
(6,5)	$(\text{TAT})_4^a, (\text{TCG})_{10}, (\text{TCG})_4\text{TC}$	10	
(9,1)	$(\text{GTC})_2\text{GT}$	1.6	
(6,4)	$(\text{GTC})_2\text{GT}$	4.7	
(5,5)	$(\text{CGT})_3\text{C}$	0.6	(PEG + PEG-DA)/DX
(6,6)	$(\text{GTT})_3\text{G}, \text{A}(\text{TTAA})_3\text{T}^a$	1.7	
(7,4)	$(\text{TCG})_4\text{TC}, (\text{GTC})_3, (\text{CCG})_4$	1.6	
(5,4)	$(\text{CGT})_3\text{C}$	0.3	
(6,5)	$(\text{TCG})_4\text{TC}, (\text{CCG})_2\text{CC}$	11	
(7,5)	$(\text{ATT})_4^a$	6.0	
(7,6)	$(\text{GTT})_3\text{G},^a (\text{GTC})_2$	0.7	
(8,3)	$(\text{TTA})_3\text{TTGTT}^a$	2.6	
(8,4)	$(\text{TATT})_2\text{TAT}$	1.5	
(10,0)	$(\text{TTA})_3\text{TTGTT}$	0.7	
(9,2)	$(\text{TGT})_4\text{T}$	1.1	
(10,2)	$(\text{AC})_{20}$	1.4	PVP-DX
(8,3)	$(\text{TCG})_4\text{TC}$	1.2	combination of PEG/PAM and PEG/DX
(7,3)	$(\text{TTA})_4\text{TT}$	2.0	combination of PVP/DX and PEG/DX

<sup>a</sup>DNA recognition sequence for the corresponding  $(n,m)$  species determined by IEX separation.<sup>5</sup>

2a. The separation procedure follows the order 1a, 2a', and repeating 2a' multiple times (Scheme 1). The absorbance spectra in Figure 2b show that multistep separation of  $(\text{GT})_{20}$ -SWCNTs enabled metal/semiconductor as well as diameter sorting. Large-diameter semiconducting (8,4) species were highly enriched in the PEG-rich top phase after the first step of separation without addition of any PVP. In the subsequent steps, increasing amounts of PVP were added to the two-phase extraction system, leading to transfer of SWCNTs into the PEG-rich top phase in a rough order of larger- to smaller-diameter semiconducting SWCNTs, leaving metallic nanotubes in the PAM-rich bottom phase in the end. The metallic mixture was further separated to yield (5,5)- and (7,4)-enriched fractions, as shown in Figure S2a,b in the Supporting Information. Similar separation results were also obtained by using  $(\text{NH}_4)_2\text{SO}_4$  in place of PVP. Interestingly, the order in which different  $(n,m)$  tubes move to the top phase is similar to the order of retention by the stationary phase in the IEX separation of  $(\text{GT})_{20}$ -SWCNTs.<sup>7</sup>

**Isolation of Single-Chirality  $(n,m)$  Species Using the PEG/PAM System.** Enrichment of single-chirality SWCNTs can also be achieved by following Scheme 1. By examining the partition of different DNA-SWCNT dispersions in the PEG/PAM system, we were able to obtain several highly enriched semiconducting SWCNT  $(n,m)$  species, the spectra of which are shown in Figure 3 and Figure S2 in the Supporting

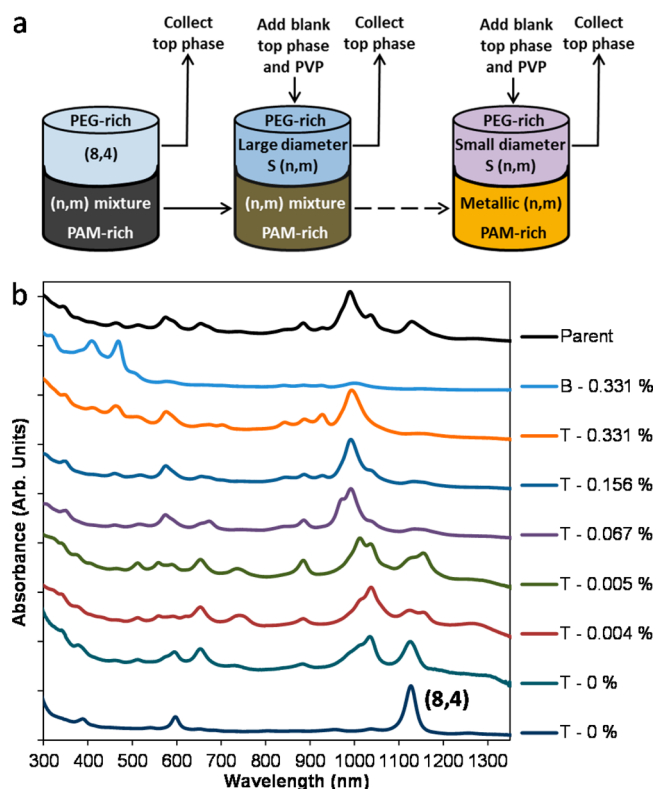


**Figure 2.** (a) Schematic illustration of the sequential addition of PVP during multistep separation of  $(GT)_{20}$ -SWCNTs in the PEG/PAM system. (b) Absorbance spectra of selected fractions with increasing concentrations of PVP. The spectra are scaled to 1 absorbance unit at the maximum  $E_{11}$  peak in each fraction. “T” denotes a top phase, “B” a bottom phase, and “S” semiconducting SWCNTs. The spectrum of the parent  $(GT)_{20}$ -SWCNT dispersion is shown at the top.

Information. Typically, the target  $(n,m)$  species were enriched in the more hydrophobic PEG-rich top phase after the first step of separation, except for  $(TAT)_4$ -SWCNTs, for which the  $(6,5)$  species was enriched in the more hydrophilic PAM-rich bottom phase. One more step of purification led to the extraction of semiconducting species  $(8,4)$ ,  $(7,5)$ ,  $(6,5)$ , and  $(9,1)$  in high purity (Figure 3). The detailed procedure for each  $(n,m)$  purification is given in the Supporting Information. In particular, the strikingly efficient two-step isolation of  $(9,1)$  species is shown in Figure S3 in the Supporting Information.

We noticed that the DNA-SWCNT loading has some effect on partition. Increased loading of DNA-SWCNTs usually led to a greater enrichment of a specific  $(n,m)$  species in the PEG-rich top phase. Since the stock DNA-SWCNT dispersions contained 0.1 mol/L NaCl, the dependence of SWCNT partition on the DNA-SWCNT loading was due at least in part to the NaCl concentration in the ATP system. Alternatively, the polyelectrolyte nature of DNA-SWCNTs may also be a cause of the observed loading effect. In this work, the final concentration of DNA-SWCNTs loaded in an ATP system was typically 0.2 times the stock concentration for SWCNTs dispersed with 40-mer DNA and 0.3 times the stock concentration for SWCNTs dispersed with shorter DNA sequences.

**Tuning of Electrostatic Interactions Using Amine-Functionalized PEG.** To mimic the separation mechanism of IEX, which enabled the identification of many DNA recognition sequences for specific SWCNT  $(n,m)$  species,<sup>5</sup> the positively charged phase-forming PEG derivative PEG-DA

was introduced into the PEG/DX system to form a (PEG + PEG-DA)-rich top phase and a DX-rich bottom phase, as shown in Figure 4a. In this case, the DNA-SWCNT loading was typically about one-third of the stock SWCNT dispersion. As expected, substantial amounts of SWCNTs were partitioned into the (PEG + PEG-DA)-rich top phase as a result of their electrostatic interactions with the positively charged PEG-DA. Depending on the DNA sequence, the amount of SWCNTs distributed into the top phase varied. Many single-chirality  $(n,m)$  species were successfully enriched by using the (PEG + PEG-DA)/DX system and following the separation procedure from 1b to 2b' shown in Scheme 1, repeating the second step several times. Most impressively, the (PEG + PEG-DA)/DX system enabled the extraction of  $(7,6)$ ,  $(7,5)$ ,  $(8,3)$ , and  $(6,6)$  species (Figure S4b–f in the Supporting Information) using the corresponding DNA recognition sequences identified previously by IEX:  $(GTT)_3G$  for  $(7,6)$ ,  $(ATT)_4$  for  $(7,5)$ ,  $(TTA)_3TTGTT$  for  $(8,3)$ ,<sup>5</sup> and  $A(TTAA)_3T$  for  $(6,6)$ .<sup>6</sup> Many other recognition sequences also allowed purification of single-chirality SWCNTs, but they did not correspond to the  $(n,m)$  tubes purified by IEX, implying that the separation procedure used for the (PEG + PEG-DA)/DX system only partially mimics the IEX mechanism. Nevertheless, the PEG-DA-induced electrostatic interaction provides an additional separation mechanism on top of the conventional hydrophobicity-based mechanism in ATP separation, demonstrating the utility of polymer functionalization in improving the ATP separation methodology.

A total of eight semiconducting SWCNT species [ $(5,4)$ ,  $(6,5)$ ,  $(8,3)$ ,  $(10,0)$ ,  $(9,2)$ ,  $(7,5)$ ,  $(8,4)$ , and  $(7,6)$ ] and three metallic species [ $(5,5)$ ,  $(6,6)$ , and  $(7,4)$ ] were effectively extracted from the parent DNA-SWCNT dispersions in the (PEG + PEG-DA)/DX system. Figure 4 shows the absorbance spectra of three purified species. Additional spectra of isolated  $(n,m)$  species are shown in Figure S4. We note that the rarely seen zigzag semiconducting  $(10,0)$  species and nonarmchair metallic  $(7,4)$  were obtained in high purity and yield by only a few steps of separation, demonstrating the effectiveness in purifying single  $(n,m)$  species by ATP separation of DNA-SWCNTs.

**Separation by Multiple ATP Systems.** To effectively purify single-chirality species, we found that sometimes it is advantageous to use one ATP system in one separation step and switch to a different ATP system in the subsequent step. Figure 5a shows an example of this strategy for the purification of  $(8,3)$  species from  $(TCG)_4TC$ -SWCNTs by tandem use of the PEG/PAM and PEG/DX systems. In the first step, the PEG/PAM system was used to extract a fraction containing an  $(8,3)$ ,  $(6,5)$ , and  $(9,1)$  mixture in the hydrophobic PEG-rich top phase. In the next step, replacing the bottom PAM phase with a fresh blank bottom phase and adding an appropriate amount of DX resulted in  $(6,5)$  enrichment in the PAM-rich bottom phase, leaving  $(8,3)$  and  $(9,1)$  in the PEG-rich top phase (Figure 5b). Adding NaSCN to the PEG-rich top phase containing the  $(8,3)$  and  $(9,1)$  mixture to drive nanotubes into the PAM-rich bottom phase for the subsequent separation step was not effective and caused loss of material due to slight aggregation at the interface. In order to obtain  $(8,3)$  species in higher yield, the mixture of  $(8,3)$  and  $(9,1)$  in the PEG-rich top phase was precipitated, resuspended in water, and transferred to a PEG/DX system. Initially, nanotubes partitioned into the hydrophilic DX-rich bottom phase. Adding an appropriate amount of PVP drove  $(9,1)$  species to the PEG-rich top phase,

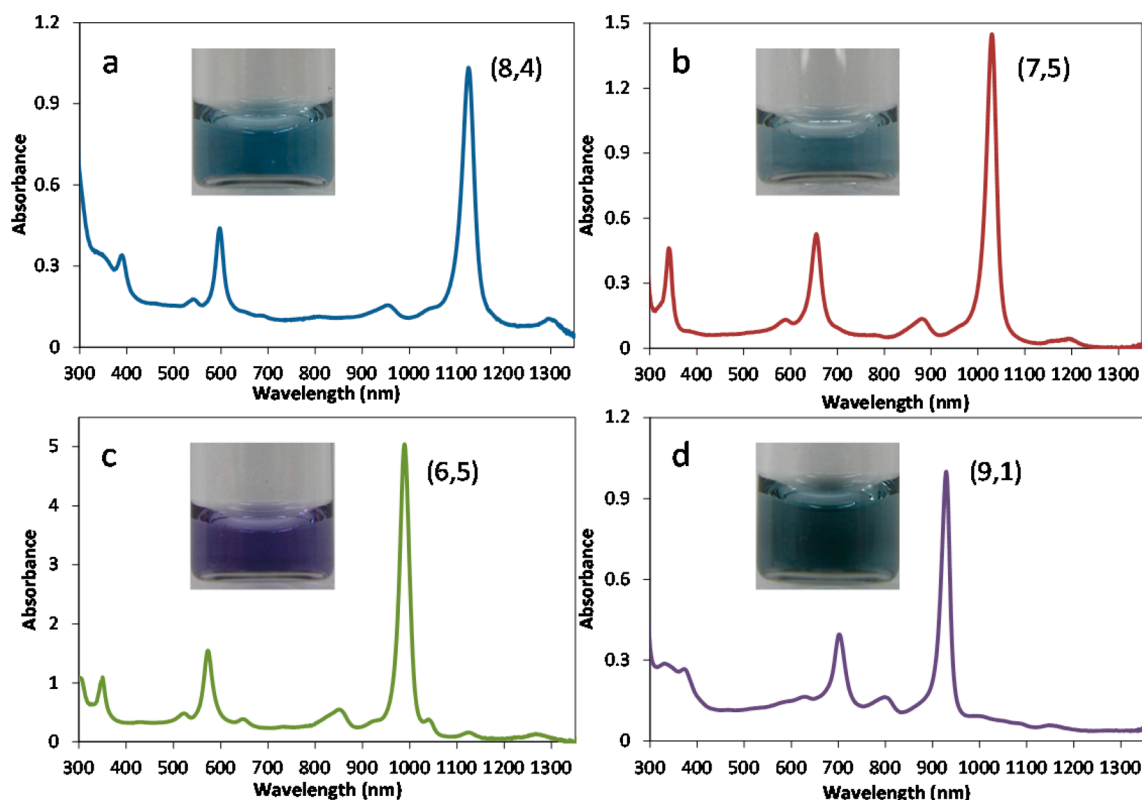


**Figure 3.** Absorbance spectra of highly enriched semiconducting  $(n,m)$  species extracted in the PEG/PAM system: (a) (8,4) from  $(GT)_{20}$ -SWCNTs; (b) (7,5) from  $(TATT)_3$ T-SWCNTs; (c) (6,5) from  $(TAT)_4$ -SWCNTs; (d) (9,1) from  $(GTC)_2$ GT-SWCNTs. The inset photograph in each panel shows the corresponding enriched  $(n,m)$  species after the original fraction was concentrated by precipitation and resuspension in water. In each spectrum, multiple optical transitions (including  $E_{11}$ ,  $E_{22}$ , and  $E_{33}$ ) of the noted chirality are clearly identifiable, with little to no contribution from any other species.

leaving the single (8,3) species in high purity in the DX-rich bottom phase. Figure 5c shows the absorbance spectrum of the purified (8,3) species. The absence of a red shift in  $E_{11}$  after multiple separation and precipitation indicates high colloidal stability of (8,3) nanotubes wrapped by the  $(TCG)_4$ TC sequence.

Another example of switching ATP systems is the purification of (7,3) nanotubes from  $(TTA)_4$ TT-SWCNTs (Figure 6). The initial ATP system used was PVP/DX, in which the top phase is PVP-rich and the bottom phase is DX-rich (Figure 6a). In the first step of separation, a (7,3)-enriched fraction was partitioned into the DX-rich bottom phase (Figure 6b), whose absorbance spectrum is shown in Figure 6c. Addition of a blank top phase of PVP/DX into the (7,3)-enriched fraction drove all of the nanotubes to the PVP-rich top phase and failed to isolate the (7,3) species. However, when the procedure from 1d to 2b' shown in Scheme 1 was followed without addition of more PVP, the system was further phase-separated into two immiscible phases: (7,3) became highly enriched in the DX-rich bottom phase, and other  $(n,m)$  impurities were moved into the PEG-rich top phase (Figure 6d).

**SWCNT Solvation Energy and ATP Separation Mechanism.** The experimental observations given above greatly expand the scope of colloidal SWCNT partition in ATP systems beyond the earlier reports for surfactant dispersions. Since SWCNT partition in an ATP system is directly determined by the SWCNT solvation energy difference between the two phases, an understanding of the separation

mechanism hinges on a quantitative account of the solvation energy in polymer-modified aqueous phases. In this section, we outline our current understanding of the factors that contribute to the solvation energy. We start by considering the free energy,  $\Delta G$ , needed to insert a rod of diameter  $D$  and length  $L$  into an aqueous solvent. The process can be viewed as composed of two steps (Scheme 2a): (1) creating a cylindrical hole of the size of the rod in the solvent and (2) putting the rod into the cylindrical hole. The free energy for step 1,  $\Delta G_1$ , can be viewed as that needed to deform the aqueous solvent. To determine how  $\Delta G_1$  scales with  $D$  and  $L$ , we follow the molecular dynamics simulation results given by Chandler,<sup>13</sup> which show that when the dimension of an inserted hole is small, the free energy for deforming a hydrogen-bonded network of water is proportional to the volume of the hole, and when the hole is larger than a critical dimension, the free energy becomes proportional to the surface area of the hole. Applying the same argument to our case, and in order to cover both small- $D$  and large- $D$  scenarios using a simple functional form, we can write  $\Delta G_1 = [a/(D + D_c)]D^2L$ , where  $a$  is a constant related to the hydrogen-bonding strength or elasticity of the aqueous solvent and  $D_c$  is a critical dimension related to the structure of the solvent. The free energy for the second step comes from the adhesion energy between the inserted rod and the aqueous solvent, which should in general be a function of  $D$ ,  $L$ , and  $(n,m)$ , so we can write  $\Delta G_2 = b(n, m, D, L)$ . Overall, we have

$$\Delta G = \frac{a}{D + D_c} D^2 L - b(n, m, D, L) \quad (1)$$

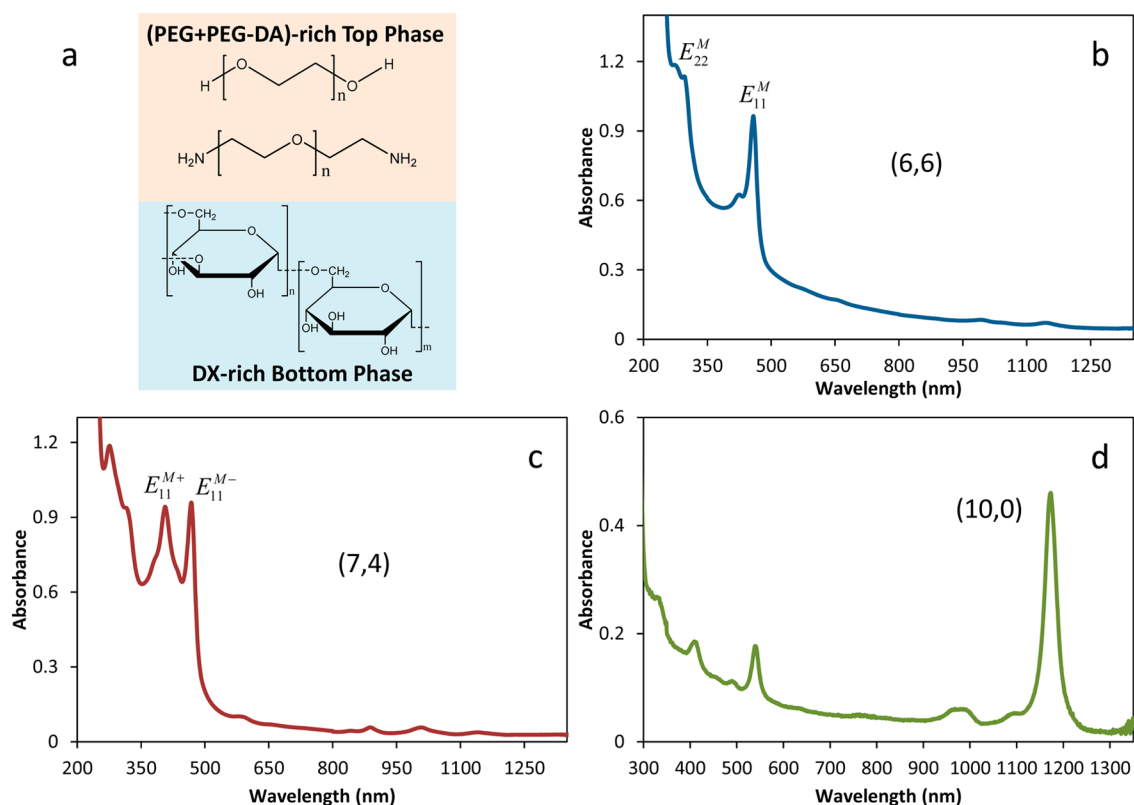


**Figure 4.** (a) Schematic illustration of the (PEG + PEG-DA)/DX system, in which the top phase is (PEG + PEG-DA)-rich and the bottom phase is DX-rich. (b–d) Absorbance spectra of highly enriched single-chirality SWCNTs extracted in the (PEG + PEG-DA)/DX system: (b) armchair metallic (6,6) from (GTT)<sub>3</sub>G-SWCNTs; (c) non-armchair metallic (7,4) from (TCG)<sub>4</sub>TC-SWCNTs; (d) zigzag (10,0) semiconducting species from (TTA)<sub>3</sub>TTGTT-SWCNTs. The spectra of metallic (6,6) and (7,4) were measured from nanotubes resuspended in water.

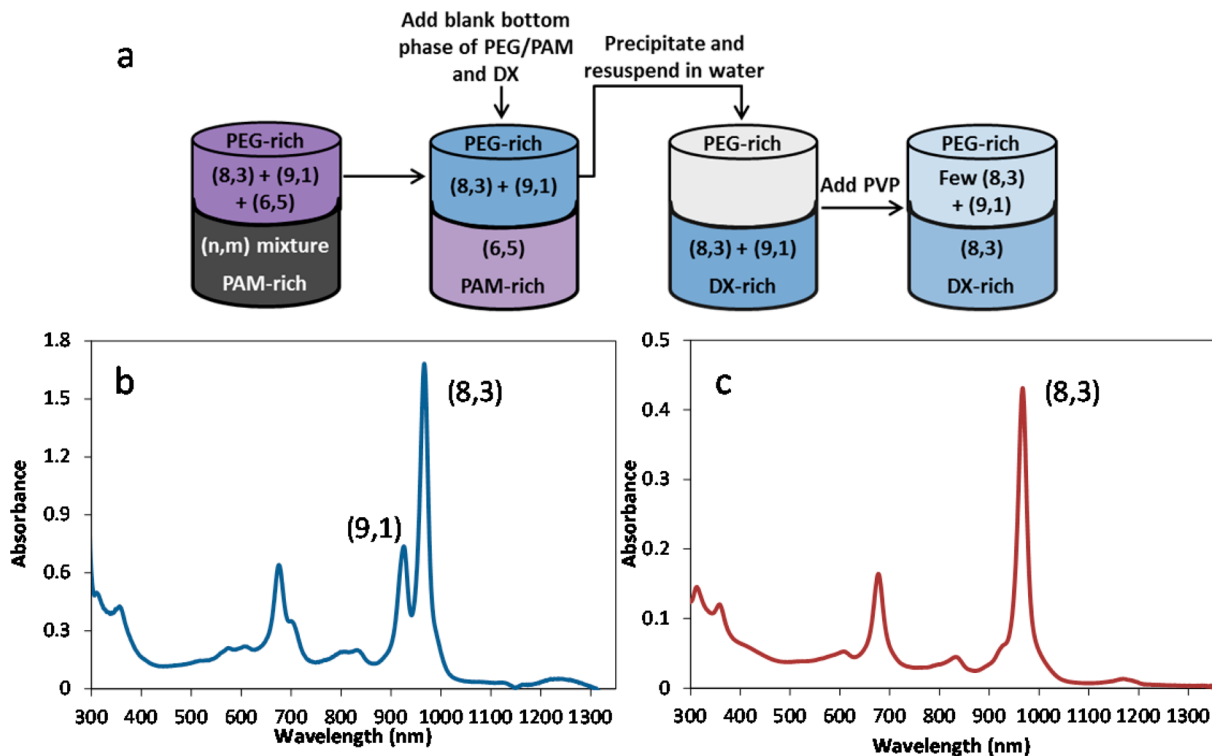


**Figure 5.** (a) Schematic illustration of single-chirality (8,3) purification by tandem use of the PEG/PAM and PEG/DX systems. (b) Absorbance spectrum of the (8,3) + (9,1) mixture obtained in the PEG-rich top phase in the PEG/PAM system. (c) Absorbance spectrum of purified (8,3) in DX-rich bottom phase after the (8,3) + (9,1) mixture was transferred into the PEG/DX system. The spectra were measured from nanotubes resuspended in water.

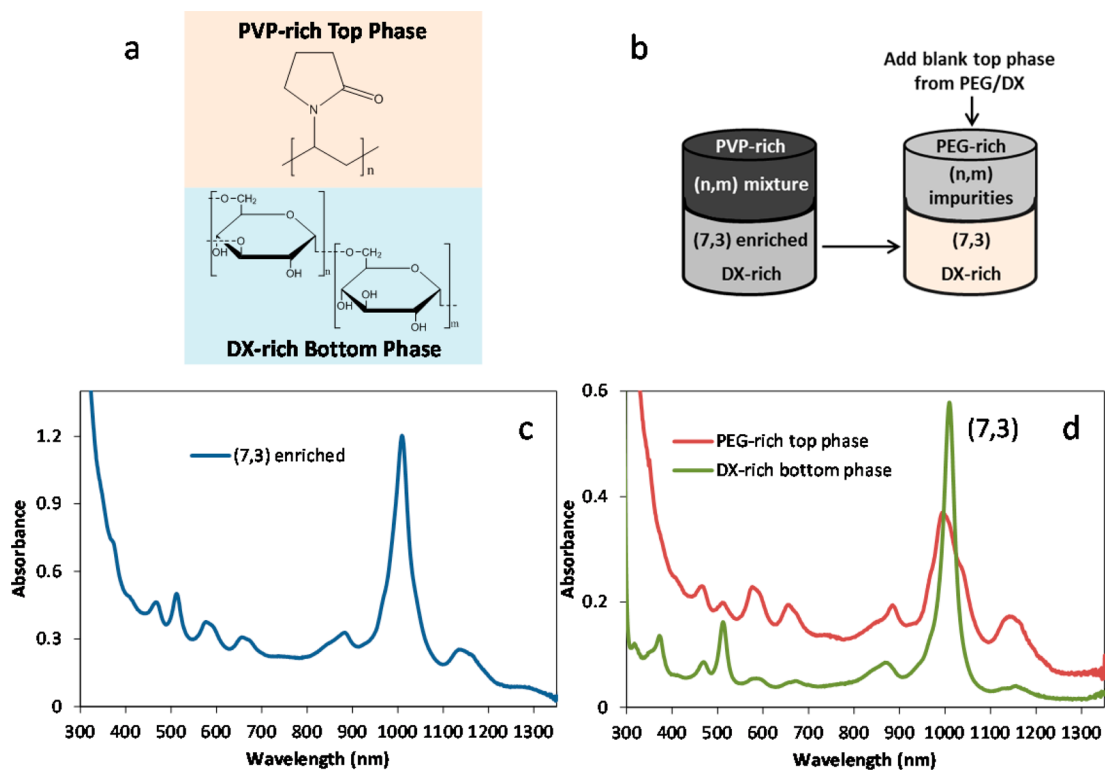
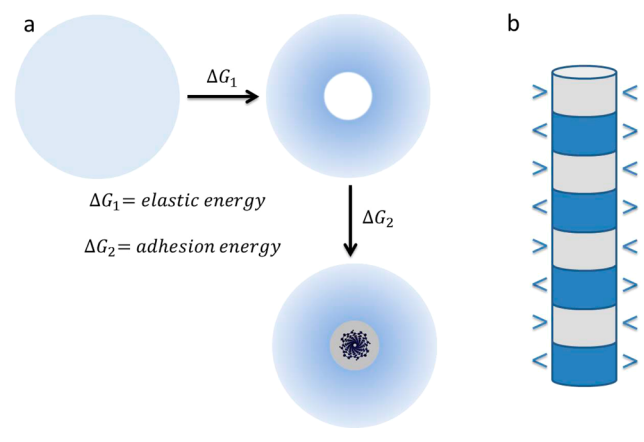


**Figure 6.** (a, b) Schematic illustrations of (a) the PVP/DX system, in which the top phase is PVP-rich and the bottom phase is DX-rich, and (b) (7,3) purification from (TTA)<sub>4</sub>TT-SWCNTs by tandem use of the PVP/DX and PEG/DX systems. (c) Absorbance spectrum of the (7,3)-enriched fraction in the DX-rich bottom phase after the first separation step in the PVP/DX system. (d) Absorbance spectra of the highly purified (7,3) nanotubes obtained from the DX-rich bottom phase and the remaining (n,m) species in the PEG-rich top phase after addition of a blank top phase of PEG/DX into the (7,3)-enriched fraction.

## Scheme 2



in which the negative sign in front of the second term signifies the reduction in free energy due to the adhesion term. We note that eq 1 resembles the free energy calculated by contact mechanics for inserting a rigid rod into a soft material, with the first term corresponding to the elastic energy and the second term to the adhesion energy.<sup>29</sup> This should come as no surprise if we view an aqueous solvent containing 10–20% polymers as a soft material.

The adhesion term in eq 1 accounts for stabilizing energies from hydrophilic interactions, an important source of which is the direct hydration of DNA-SWCNTs. Ideas for calculating the hydration energy can be found in the literature.<sup>30,31</sup> Here we apply these ideas to colloidal SWCNTs. For the

convenience of our discussion, we assume that the aforementioned rod has a periodic variation in surface functionalities along its axis, denoted in Scheme 2b by blue rings for hydrophilic areas and gray rings for hydrophobic areas. We use blue “>” and “<” shapes to represent water molecules near the rod and their ordering by the surface functionalities. The detailed configuration of the hydration layer affects the calculation of the hydration energy, since nearby hydrogen bonds can be either mutually constructive or destructive depending on the relative configuration.<sup>31</sup> Another way to look at this is that the undulating pattern of hydrophilic/hydrophobic functionalities determines the energetic cost of deformation of the water structure beyond the hydration layer.<sup>30</sup> In this view, the adhesion energy contains an elastic component, and dividing the solvation energy into two terms in eq 1 is merely for the convenience of discussion. In the case of DNA-SWCNTs, the undulating pattern is presumably determined by the DNA sequence and the SWCNT chirality (n,m). DNA-controlled SWCNT partition is thus a consequence of the sensitive dependence of the hydration energy on the exact spatial distribution of hydrophilic groups. In the case of surfactant-dispersed SWCNTs, randomness in the surfactant coating structure may smooth out any surface undulation effect on hydration energy, leaving the overall solvation energy primarily dependent on *D*, *L*, and the metal/semiconductor character of the SWCNT.

Another source of the adhesion energy is the stabilization energy of a negatively charged DNA-SWCNT in a high-dielectric aqueous solvent, which can be expressed as a function of the linear charge density, the geometry of the DNA-



SWCNT, and the ionic strength of the solvent. Additional electrostatic interactions between DNA-SWCNTs and charged polymers (PEG-DA) in one of the two phases may further elevate the effect of the adhesion term on SWCNT partition. A complication to the simple electrostatic picture is the observed specific salt effect on DNA-SWCNT partition. At the experimental level, modulation of DNA-SWCNT partition is crucial for achieving single ( $n,m$ ) purification. The opposite effects of chaotropic salts (e.g., NaSCN) and kosmotropic salts (e.g., Na<sub>2</sub>CO<sub>3</sub>, Na<sub>2</sub>SO<sub>4</sub>) on DNA-SWCNT partition imply that simple electrostatic considerations are not sufficient to account for the experimental observations. We suggest that the salt modulation effect results from modification of the aqueous solvent structure, which in turn changes the hydrophobic term (the first term in eq 1) and the hydration interaction term (the second term in eq 1).

How do we understand the role of other modulators, such as PVP, pH, and temperature, in the context of the mechanistic discussion given above? We note that DNA-SWCNT partition is the result of a competition between two polymer phases in terms of the solvation free energy given by eq 1. Broadly speaking, any factor that perturbs the physicochemical properties of one phase relative to the other results in modulation of the partition. This might be the cause for the observed effects of pH and temperature. The strong modulating effect of PVP is not clearly understood. PVP may act as a dispersant to compete with DNA for SWCNT binding and/or engage in electrostatic interactions with DNA-SWCNTs. More work is needed to clarify the mechanism of PVP modulation of DNA-SWCNT partition in polymer two-phase systems.

## SUMMARY AND FUTURE PERSPECTIVE

This work represents our first attempt to extend the ATP method to the separation of DNA-SWCNTs. The surfactant-free nature of DNA-SWCNT dispersions makes many polymer-modified aqueous phases useful for extraction. A few polymer systems have been tested in the current study, and many more are potentially useful and waiting to be tested. Our observations clearly demonstrate DNA sequence-dependent partition of SWCNTs in aqueous phases. Although only a small number of DNA sequences from the huge ssDNA library were tested in this work, we were still able to purify many single-chirality ( $n,m$ ) species. The wide selection of polymer phases and the availability of practically unlimited number of DNA sequences therefore suggest that there is tremendous potential for further improvement in SWCNT separation by this methodology. This is a unique advantage of our approach in comparison with other separation methods. Our analysis suggests that *hydration energy is sensitively dependent on the exact spatial distribution of hydrophilic groups*. While this point might not be new to biochemists and biophysicists, it is demonstrated in a strikingly clear way by our studies. Future work will continue to pursue mechanistic and quantitative understanding of the rich and tractable phenomena shown by DNA-SWCNT partition in polymer-modified aqueous phases.

## ASSOCIATED CONTENT

### Supporting Information

Separation of DNA-SWCNTs in ATP systems, estimated yield for each purified ( $n,m$ ) species, purification of single-chirality ( $n,m$ ) species using the PEG/PAM and (PEG + PEG-DA)/DX systems, purification of (10,2) species using the PVP/DX system, and purification of (8,3) species by tandem use of the

PEG/PAM and PEG/DX systems. This material is available free of charge via the Internet at <http://pubs.acs.org>.

## AUTHOR INFORMATION

### Corresponding Author

ming.zheng@nist.gov

### Notes

The authors declare no competing financial interest.

## ACKNOWLEDGMENTS

We thank Drs. Jeffrey Fagan, Anand Jagota, Jeetain Mittal, and Jack Douglas for their critical comments on the manuscript. G.A. acknowledges postdoctoral fellowship support from the National Research Council.

## REFERENCES

- (1) Khripin, C. Y.; Fagan, J. A.; Zheng, M. *J. Am. Chem. Soc.* **2013**, *135*, 6822.
- (2) Fagan, J. A.; Khripin, C. Y.; Silvera Batista, C. A.; Simpson, J. R.; Házroz, E. H.; Hight Walker, A. R.; Zheng, M. *Adv. Mater.* **2014**, *26*, 2800.
- (3) Subbaiyan, N. K.; Cambré, S.; Parra-Vasquez, A. N. G.; Házroz, E. H.; Doorn, S. K.; Duque, J. G. *ACS Nano* **2014**, *8*, 1619.
- (4) Zhang, M.; Khripin, C. Y.; Fagan, J. A.; McPhie, P.; Ito, Y.; Zheng, M. *Anal. Chem.* **2014**, *86*, 3980.
- (5) Tu, X.; Manohar, S.; Jagota, A.; Zheng, M. *Nature* **2009**, *460*, 250.
- (6) Tu, X.; Hight Walker, A. R.; Khripin, C. Y.; Zheng, M. *J. Am. Chem. Soc.* **2011**, *133*, 12998.
- (7) Zheng, M.; Jagota, A.; Strano, M. S.; Santos, A. P.; Barone, P.; Chou, S. G.; Diner, B. A.; Dresselhaus, M. S.; Mclean, R. S.; Onoa, G. B.; Samsonidze, G. G.; Semke, E. D.; Usrey, M.; Walls, D. J. *Science* **2003**, *302*, 1545.
- (8) Zheng, M.; Jagota, A.; Semke, E. D.; Diner, B. A.; McLean, R. S.; Lustig, S. R.; Richardson, R. E.; Tassi, N. G. *Nat. Mater.* **2003**, *2*, 338.
- (9) Liu, H.; Nishide, D.; Tanaka, T.; Kataura, H. *Nat. Commun.* **2011**, *2*, 309.
- (10) Nish, A.; Hwang, J.-Y.; Doig, J.; Nicholas, R. J. *Nat. Nanotechnol.* **2007**, *2*, 640.
- (11) Arnold, M. S.; Green, A. A.; Hulvat, J. F.; Stupp, S. I.; Hersam, M. C. *Nat. Nanotechnol.* **2006**, *1*, 60.
- (12) Albertsson, P. A. *Partition of Cell Particles and Macromolecules*, 2nd ed.; Wiley-Interscience: New York, 1971.
- (13) Chandler, D. *Nature* **2005**, *437*, 640.
- (14) Ashbaugh, H. S.; Pratt, L. R. *Rev. Mod. Phys.* **2006**, *78*, 159.
- (15) Mace, C. R.; Akbulut, O.; Kumar, A. A.; Shapiro, N. D.; Derda, R.; Patton, M. R.; Whitesides, G. M. *J. Am. Chem. Soc.* **2012**, *134*, 9094.
- (16) Zaslavsky, B. Y. *Aqueous Two-Phase Partitioning*; Marcel Dekker: New York, 1994.
- (17) Ortiz-Acevedo, A.; Xie, H.; Zorbaz, V.; Sampson, W. M.; Dalton, A. B.; Baughman, R. H.; Draper, R. K.; Musselman, I. H.; Dieckmann, G. R. *J. Am. Chem. Soc.* **2005**, *127*, 9512.
- (18) Grigoryan, G.; Kim, Y. H.; Acharya, R.; Axelrod, K.; Jain, R. M.; Willis, L.; Drndic, M.; Kikkawa, J. M.; DeGrado, W. F. *Science* **2011**, *332*, 1071.
- (19) Roxbury, D.; Zhang, S.-Q.; Mittal, J.; DeGrado, W. F.; Jagota, A. *J. Phys. Chem. C* **2013**, *117*, 26255.
- (20) O'Connell, M. J.; Boul, P.; Ericson, L. M.; Huffman, C.; Wang, Y.; Haroz, E.; Kuper, C.; Tour, J.; Ausman, K. D.; Smalley, R. E. *Chem. Phys. Lett.* **2001**, *342*, 265.
- (21) Roxbury, D.; Tu, X.; Zheng, M.; Jagota, A. *Langmuir* **2011**, *27*, 8282.
- (22) Roxbury, D.; Jagota, A.; Mittal, J. *J. Am. Chem. Soc.* **2011**, *133*, 13545.
- (23) Roxbury, D.; Mittal, J.; Jagota, A. *Nano Lett.* **2012**, *12*, 1464.
- (24) Roxbury, D.; Jagota, A.; Mittal, J. *J. Phys. Chem. B* **2013**, *117*, 132.

- (25) Khripin, C. Y.; Arnold-Medabalimi, N.; Zheng, M. *ACS Nano* **2011**, *5*, 8258.
- (26) Lo Nostro, P.; Ninham, B. W. *Chem. Rev.* **2012**, *112*, 2286.
- (27) Duque, J. G.; Cognet, L.; Parra-Vasquez, A. N. G.; Nicholas, N.; Schmidt, H. K.; Pasquali, M. *J. Am. Chem. Soc.* **2008**, *130*, 2626.
- (28) Worley, J. D.; Klotz, I. M. *J. Chem. Phys.* **1966**, *45*, 2868.
- (29) Style, R. W.; Hyland, C.; Boltyanskiy, R.; Wettlaufer, J. S.; Dufresne, E. R. *Nat. Commun.* **2013**, *4*, 2728.
- (30) Marčelja, S.; Radić, N. *Chem. Phys. Lett.* **1976**, *42*, 129.
- (31) Ben-Naim, A. *Molecular Theory of Water and Aqueous Solutions Part II: The Role of Water in Protein Folding, Self-Assembly and Molecular Recognition*; World Scientific: Singapore, 2011.